Source contamination, crustal assimilation, and magmatic recycling during three flare-ups in the Cretaceous Peruvian Coastal Batholith

LOMA LINDA UNIVERSITY

CALIFORNIA STATE UNIVERSITY LONG BEACH

Ana María Martínez Ardila[1], Lance Pompe[1], Benjamin Clausen[1 2], Scott Paterson, Gregory J. Holk[3], Peter Luffi[4 5]

[1]Department of Earth and Biological Sciences, Loma Linda University, Loma Linda, California; [2] Geoscience Research Institute, Loma Linda, California USA; [3] Department of Geological Sciences, California State University, Long Beach USA; [4] Sabba Stefanescu Institute of Geodynamics, Bucharest, Romania, [5] Geological Institute of Romania, Bucharest, Romania

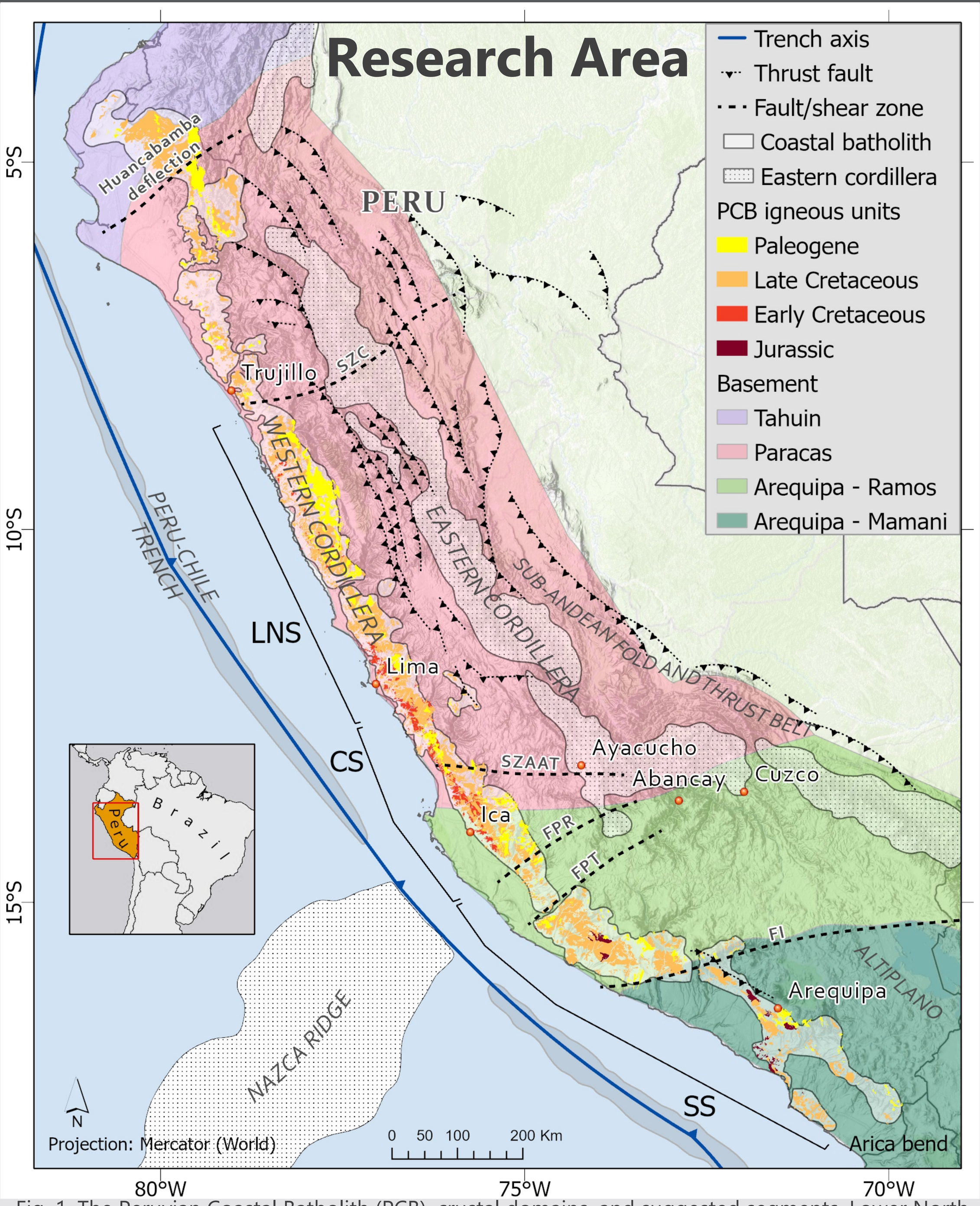

Fig. 1. The Peruvian Coastal Batholith (PCB), crustal domains, and suggested segments. Lower North Segment (LNS), Central Transitional Segment (CS), and South Segment (SS). Patacancha-Tambuco Fault (FPT), Puyentimary Fault (FPR), Iquipi Fault (FI), Contaya Shear Zone (CSZ), Shear Zone Abancay-Andahuaylas (SZAAT).

Summary

To understand better continental arcs and their evolution we must consider several topics such as the magma sources and mechanisms of compositional diversity, causes of flare-ups and lulls, spatial and temporal variations, and tectonic processes driving arc evolution. This research addresses the origin of along-arc chemical changes observed in the PCB by using an up-to-date geochemical and geochronological database in order to: 1) assess the evidence for proposed chemical trends, 2) to examine spatial and temporal changes along the PCB segments, and 3) relate these to the tectonic setting, subduction parameters, magma sources, and crustal assimilation processes. Our results show a non-steady-state pattern over variable temporal and spatial scales and that chemical diversity along and across the arc is the result of the extent of differentiation, assimilated materials, basement type, changes in crustal thickness, arc migration, changes in mantle input, and transitioning from depleted to lithospheric mantle. In order to explain the causes of flare-ups and arc chemical diversity in the PCB we suggest that coupling of external (lower plate) and internal (upper plate) processes in complex ways at different spatial and temporal scales form the final arc diversity.

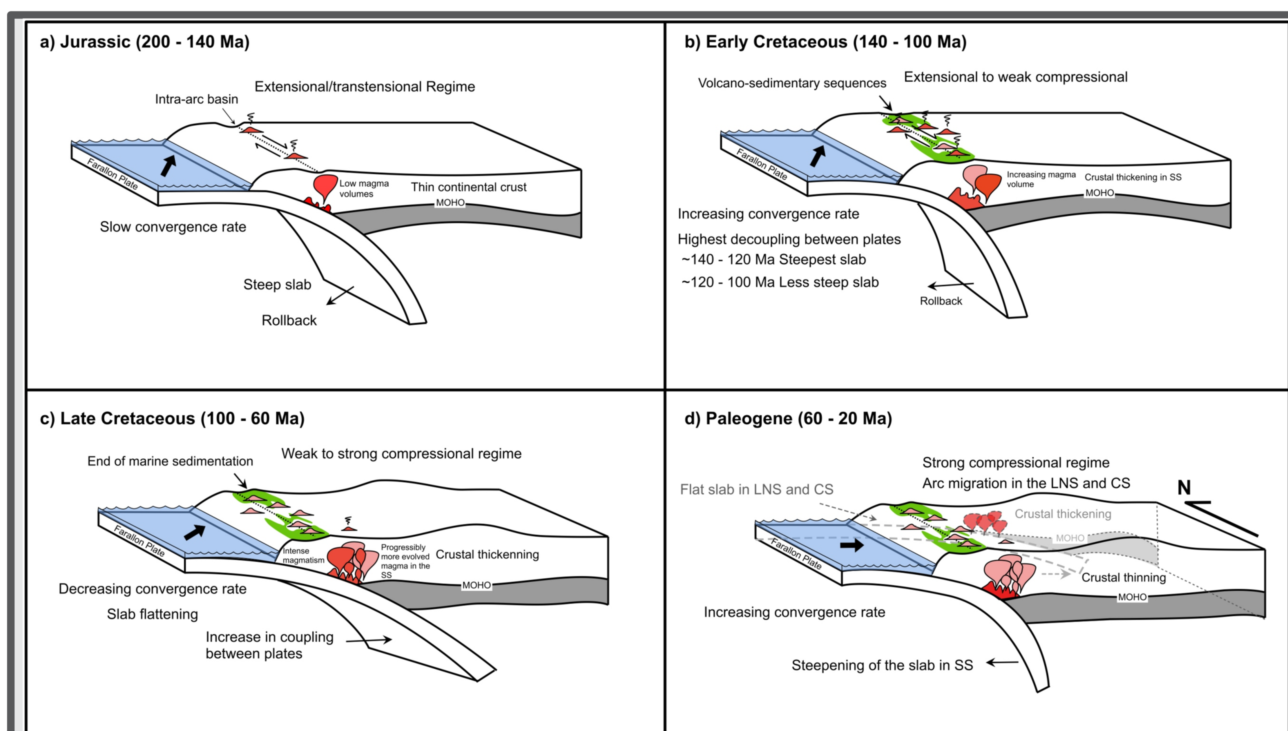

Fig. 2. Tectono-magmatic Evolution of W Peru. (a) Jurassic: transtensional to extensional controlled by the absolute motion of the upper plate, slow CR and reduced magmatism. (b) Early Cretaceous: transition from extensional to weak compressional, the onset of the Andean orogeny with increasing magmatism, and marine transgressions. (c) Late Cretaceous: transition from weak compressional to strong compressional with decreasing CR, slab flattening, increasing plate coupling, and intense magmatism. (d) Paleogene: increasing convergence rates, strong compressional, low magmatism and contrasting behavior between north (flat slab, crustal thinning) and south (steepening slab, crustal thickening).

Geologic Setting

The PCB is represented by Lower Jurassic to Upper Eocene calc-alkaline granitoids located in the Western Cordillera (WC).

Cretaceous basins in the WC were intruded by the early plutons of the PCB (Atherton et al., 1983; De Haller et al., 2006). The basement for the basins and the PCB in the south is the Mesoproterozoic Arequipa terrane (Casquet et al., 2010; Loewy et al., 2004).

To the north, there are no exposures of basement but offshore studies identified a Precambrian basement underlying the Paracas terrane (Romero et al., 2013). The south-to-north and west-to-east chemical variation of the PCB was used to propose the PCB segments (Cobbing and Pitcher, 1972).

Recently, Ccallo Morocco et al. (2021) suggested three: Piura, Lima, and Arequipa, and two transition zones between segments: Trujillo-Chiclayo and Chaparra-Caraveli. The boundaries between PCB segments coincide with ancient fault zones where rifting during the Permo-Triassic and the Jurassic controlled basin formation, magmatism, and mineralization.

Geochronology

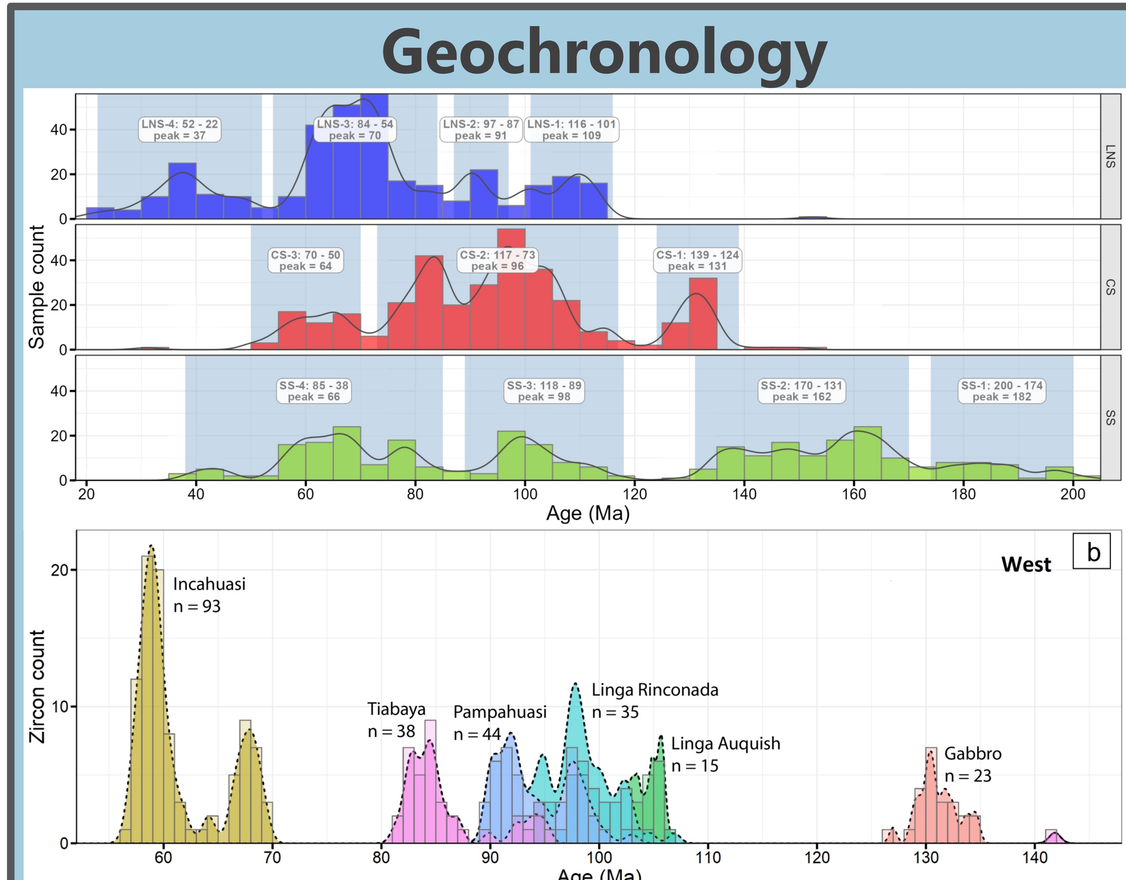

Fig. 3. a. Igneous bedrock age spectra histogram depicting flare-ups across the LNS, CS, and SS. The sample ages are a combination of measured U–Pb ages and K–Ar, Rb–Sr, Ar–Ar. b. Igneous bedrock U–Pb age spectra of 248 individual zircons from 9 samples collected from the PCB near Ica.

U-Pb zircon age display along-arc variation in the timing of increased magmatic activity, where the oldest flare-up started in the SS (~200–174 Ma) and a late Paleogene flare-up (~52–22 Ma) identified in the LNS. The S to N trend represents a W to E migration of the arc as well. Flare-ups progressing north are temporally offset (not continuous) between neighboring segments. We defined 4 flare-ups for the SS from ~200 to 38 Ma, 3 flare-ups for the CS from ~139 to 50 Ma, and 3 flare-ups for the LNS from ~116 to 22 Ma.

Geochemistry

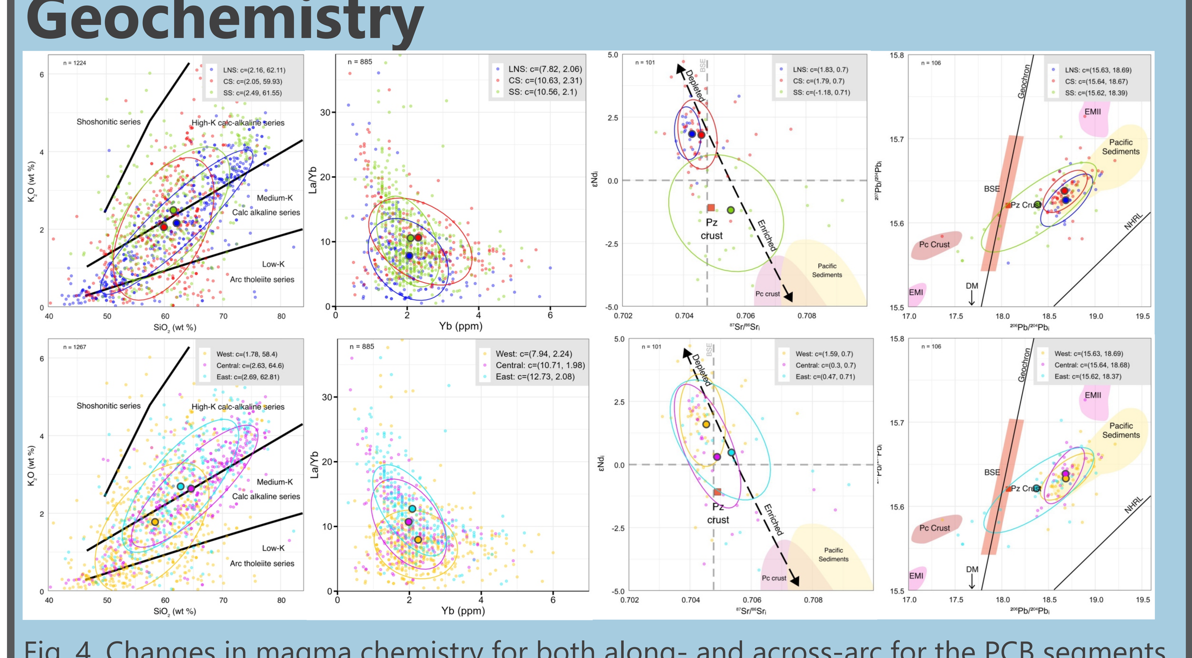

Fig. 4. Changes in magma chemistry for both along- and across-arc for the PCB segments. Datasets includes plutonic and associated volcanic rocks.

The PCB chemical signature is calc alkaline. The chemical changes along-arc segments, from S to N, characterized by a S to N decrease of the following proxies: K_2O (2.5 to 2.13 wt%), La/Yb (10.58 to 7.84), Sri (0.758 to 0.704), and $\delta^{18}O$(8.85 to 8.38).

The SS is different from the LNS. The CS is a transitional zone between the LNS and SS, because it exhibits gradual changes for most of the chemical values and the highest values of Pb isotopes. A general trend from W to E is the decrease in εNd, and 206Pb/204Pb, and an increase of K_2O, La/Yb, Sri, and $\delta^{18}O$.

Synthesis of Datasets

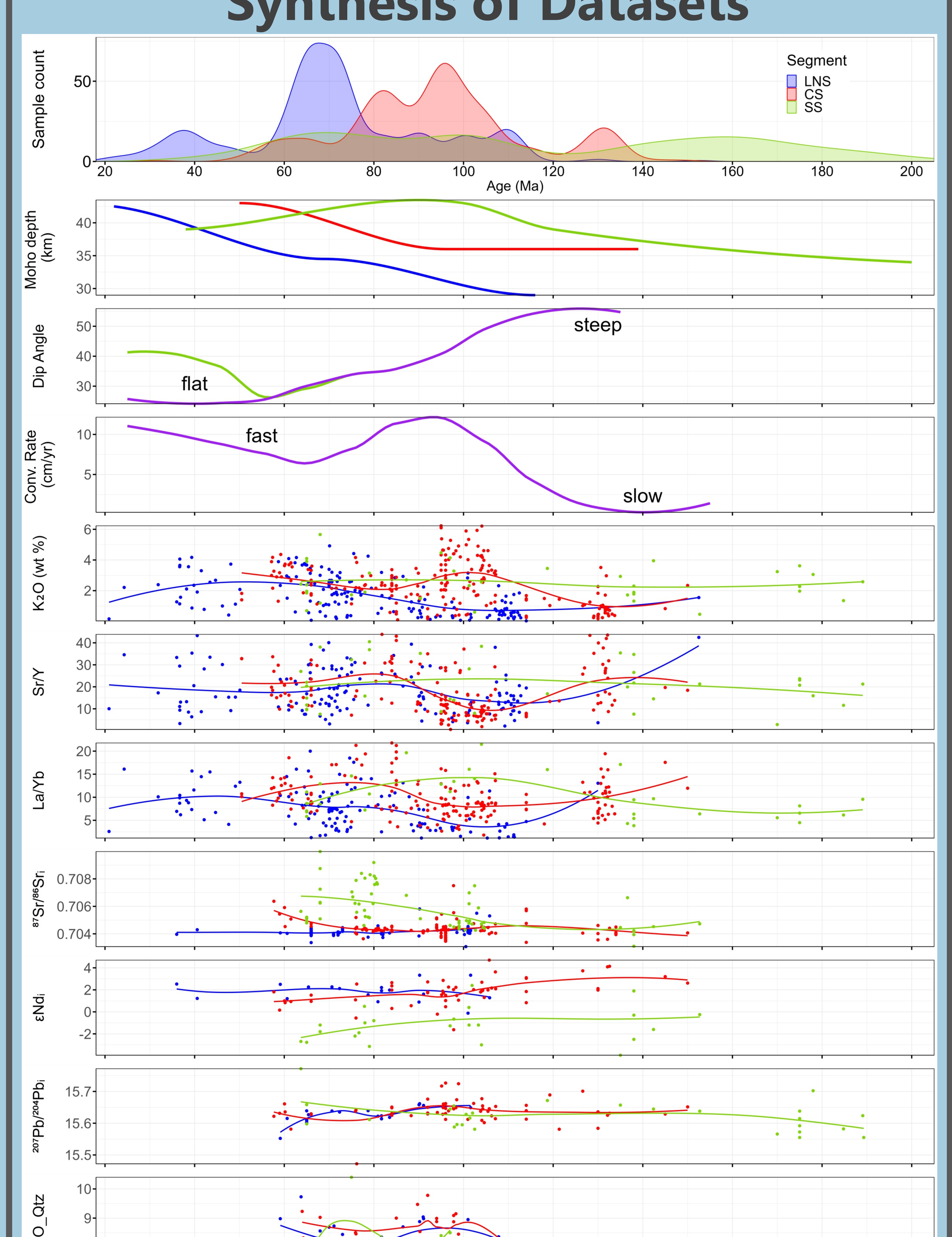

Fig. 5. Age histogram and whole-rock petrogenetic indicators. All geochemical parameters are plotted according to the outcrop age. Data source includes our new age and chemical data and compiled whole rock data (Supplementary Data): South Segment (SS), Central Transitional Segment (CS), and Lower Northern Segment (LNS).

Statistical analyses were run on the datasets to calculate the mean for identifying trends and evaluate the boundaries for each segment. This approach revealed along-arc variation during periods of increased magmatic activity, where flare-ups are temporally offset between neighboring segments. Older flare-ups started first in the SS and from S to N there is a decrease of K_2O, La/Yb, Sri, and $\delta^{18}O$ and an increase of eNd.

Moho depth estimates were obtained following the method outlined by Luffi and Ducea (2022). Crustal thickness evolution from south to north as follows: (1) the SS thickens from 34 km at ~200 Ma to 43 km at ~89 Ma and then thins to 39 km at ~60 Ma; (2) the CS starts with a thickness of 36 km at ~139-73 Ma and then to 43 km at ~60 Ma; (3) the LNS shows a constant thickness of 29 km at ~116-87 Ma and then thickening from 34.5 km at ~84 Ma to 42.5 km at ~22 Ma.

In summary, crust for the LNS and CS was thinner and thickened during the late Cretaceous and into the early Cenozoic. The SS was different because a thinning episode started in the late-Cretaceous and continued until the late-Eocene (~85-38 Ma).

AFC Modeling

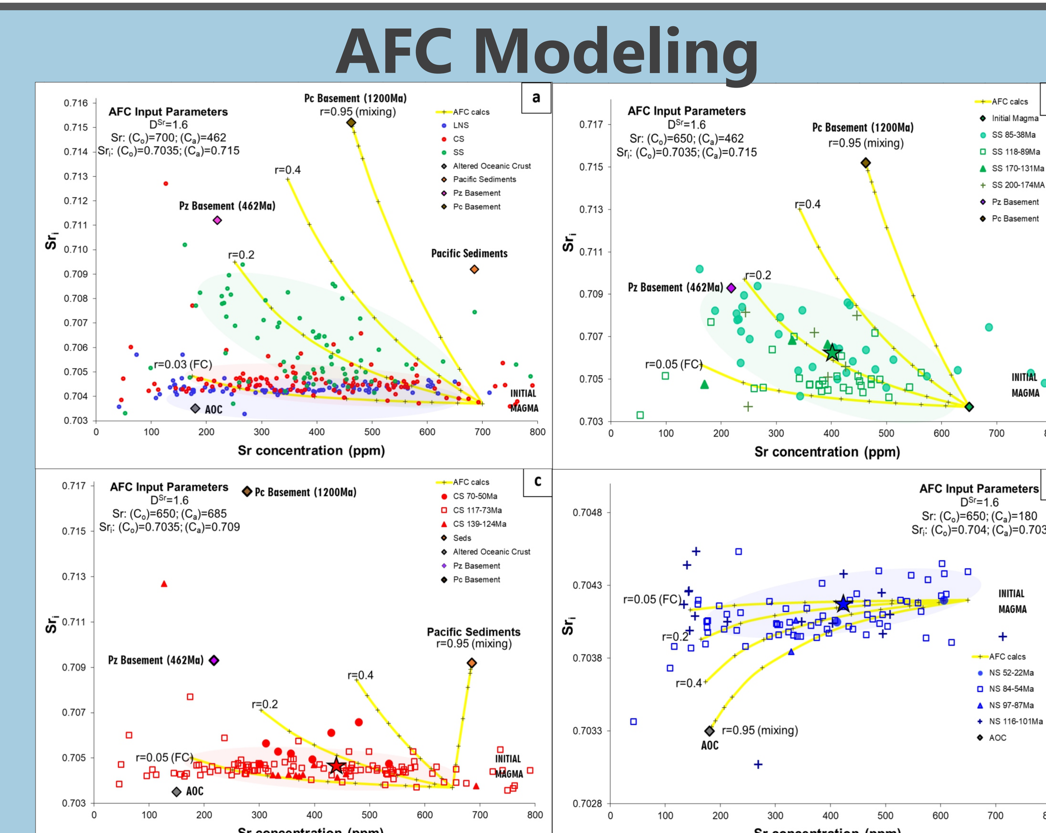

Fig. 6. The initial magma uses a Sri and Sr values for parental mantle (Gale et al., 2003; Faure, 2009). Color fields represent the distribution of the samples, and the star symbol indicates their respective averages. (a) Higher assimilation of Pc crust in the SS. The maximum amounts of crust assimilated to form the arcs are: (b) 25% Pc with minor Pz crust for the SS; (c) 10–15% for AOC (Altered Oceanic Crust) and 10% Pacific sediments (PS) for CS, and (c) an average of 30% AOC for LNS.

SS: Parental mantle magmas assimilated ~20–25% of Pc crust at the emplacement level. Possibly minor contamination from Pz crust and PS in the source. Assimilation is lower during the 118–89 Ma episode and increases with the younger 85–38 Ma flare-up.

CTS: Parental mantle magmas interacted with three assimilants: (1) PS ~5–10% in the source region, (2) AOC basement ~10–15%, and (3) minor Pc and Pz crustal assimilation during fractional crystallization. The assimilation of isotopically evolved materials increased through time reaching a maximum at 70–50 Ma.

LNS: Contamination of parental magmas in this segment resulted from a less evolved end member characterized by low Sr and Sri values (Fig. 6c). ~20–30% assimilation derived from AOC and took place during fractional crystallization.

Causes of Chemical Diversity

The along-arc trend in the PCB from south to north can be explained by four factors: (1) interaction of magmas with two basement types, i.e., the Arequipa continental crust or the Paracas attenuated continental crust covered by mafic pillow lavas and pyroclastic rocks interfingered with marine sediments, (2) variation of assimilation at emplacement levels associated with changes in crustal thickness, (3) a changing amount of subducted sediment assimilated at the magma source, and (4) the nature of the mantle reservoir.

Magmas experienced <20–30% crustal assimilation, implying that the majority of these magmas are mantle-derived. Granitoids in the SS of the PCB have been modified by magmas rising through the Arequipa terrane assimilating Pc and Pz basement.

The high Pb isotope ratios in the CS supports the interpretation that both basement and subducted PS were assimilated into the mantle magmas (Martínez Ardila et al., 2019; Mukasa, 1986).

Accross-arc trends suggest that the arc migrated to the east through time. An increase in assimilation as the arc migrates to the east can be predicted by crustal thickening, but the isotopically evolved signatures can be linked to partial melting of the mantle.

Modern overview of the PCB

(1)The PCB shows non-steady-state pattern of magmatism at variable temporal and spatial scales. Some flare-ups are discrete, but others are synchronous for hundreds of kilometers along-arc and a periodicity of 30–40 m.y.

(2)The identified chemical diversity both along- and across-arc are the result of changing upper plate mantle input (transitioning from depleted to lithospheric mantle), types of upper plate basement (i.e., Paracas and Arequipa terranes), varying types and degrees of assimilated material from Pacific sediments, changing crustal thickness, arc migration, and the extent of magma fractionation.

(3)We find no convincing correlations between arc chemistry and plate motion. However, upper plate tectonic phenomena, such as styles of tectonics (extension, contraction, transpression) and/or crustal thickness may show weak relationships to geochemical signals, although it is typically hard to fully separate different tectonic effects from other parameters such as mantle and basement type.

(4)We recognize a complex interplay between external and internal processes. External processes controlling fairly instantaneous boundary conditions for arc behavior while upper plate processes are influenced by lengthy composite histories of continental margins. The spatial and temporal variability in the PCB signals an equivalent variability in flare-up triggers. However much of our geochemical data and modeling point towards the importance of episodic mantle processes playing the dominant role in triggering flare-ups.

(5)We document the incredible heterogeneity of both tectonic and magmatic arc behavior over short spatial lengths. Therefore, the causes also have to be heterogeneous over these length scales. This complexity must reflect a dynamic interaction between lower plate driven boundary conditions on upper plate long term evolution of mantle, crustal basement and evolving magma systems.

This poster is based on a full paper. See link to access the full paper https://www.sciencedirect.com/science/article/pii/S0024493723002827?via%3Dihub

Acknowledgements

The authors acknowledge financial support for this study from Loma Linda University and the Geoscience Research Institute (Projects GRI2014-BC01 and GRI2015-AM10). We thank Orlando Poma for his valuable assistance during fieldwork. We thank the lab scientists at the Arizona LaserChron Center and support from NSF grant EAR 1649254. We are especially grateful to the Bendezu Family for their kindness and hospitality during our visits to Peru. Martínez-Ardila thanks Felipe Pichinual for data synthesis and drafting help, Luiz Pereira and Alex Voos for helping with data compilation.

References

Atherton, M. P., Pitcher, W. S., Warden, V. (1983). The Mesozoic marginal basin of central Peru. Nature, 305(5932), 303-306.

Ccallo Morocco, W. E., López Aguilar, Y. P., Guo, W., Liu, J., Chen, S., Duan, Z. (2021). Características litogeoquímicas y petrográficas en los bordes norte y sur del segmento Lima-Batolito de la Costa, comparada con el sureste de China-[Boletín D 35].

De Haller, A., Corfu, F., Fontboté, L., Schaltegger, U., Barra, F., Chiaradia, M., Alvarado, J. Z. (2006). Geology, geochronology, and Hf and Pb isotope data of the Raúl-Condestable IOCG deposit, central coast of Peru. Economic Geology, 101(2), 281-310.

Loewy, S. L., Connelly, J. N., Dalziel, I. W. (2004). An orphaned basement block: The Arequipa-Antofalla Basement of the central Andean margin of South America. Geological Society of America Bulletin, 116(1-2), 171-187.

Martínez-Ardila, A. M., Paterson, S. R., Memeti, V., Parada, M. A., Molina, P. G. (2019). Mantle driven Cretaceous flare-ups in Cordilleran arcs. Lithos, 326, 19-27.

Mukasa, S. B. (1986). Common Pb isotopic compositions of the Lima, Arequipa and Toquepala segments in the Coastal batholith, Peru: implications for magmagenesis. Geochimica et Cosmochimica Acta, 50(5), 771-782.

Romero, D., Valencia, K., Alarcón, P., Peña, D., Ramos, V. A. (2013). The offshore basement of Perú: Evidence for different igneous and metamorphic domains in the forearc. Journal of South American Earth Sciences, 42, 47-60.